entropy

MDPI

Article

# Multiscale Cross-Approximate Entropy Analysis of Bilateral Fingertips Photoplethysmographic Pulse Amplitudes among Middle-to-Old Aged Individuals with or without Type 2 Diabetes

**Hsien-Tsai Wu [1], Cheng-Chan Yang [1,2], Gen-Min Lin [1,3,4,*], Bagus Haryadi [1,5], Shiao-Chiang Chu [1], Chieh-Ming Yang [1] and Cheuk-Kwan Sun [6,*]**

1 Department of Electrical Engineering, National Dong-Hwa University, Hualien 97401, Taiwan; hsientsaiwu@gmail.com (H.-T.W.); joseph9204@yahoo.com.tw (C.-C.Y.); 810523004@gms.ndhu.edu.tw (B.H.); 610523004@gms.ndhu.edu.tw (S.-C.C.); j82887@gmail.com (C.-M.Y.)
2 Department of Traditional Chinese Medicine, Buddhist Tzu-Chi General Hospital, Hualien 970, Taiwan
3 Departments of Medicine, Hualien Armed Forces General Hospital, Hualien 970, Taiwan
4 Tri-Service General Hospital, National Defense Medical Center, Taipei 114, Taiwan
5 Department of Physics, Universitas Ahmad Dahlan, Yogyakarta 55164, Indonesia
6 Department of Emergency Medicine, E-Da Hospital, I-Shou University, Kaohsiung 840, Taiwan
* Correspondence: farmer507@yahoo.com.tw (G.-M.L.); lawrence.c.k.sun@gmail.com (C.-K.S.); Tel.: +886-03-862-0601 (G.-M.L.); +886-07-615-0011 (C.-K.S.); Fax: +886-03-862-1370 (G.-M.L.); +886-07-615-0915 (C.-K.S.)

Academic Editor: Herbert Jelinek
Received: 30 January 2017; Accepted: 28 March 2017; Published: 30 March 2017

**Abstract:** Multiscale cross-approximate entropy (MC-ApEn) between two different physiological signals could evaluate cardiovascular health in diabetes. Whether MC-ApEn analysis between two similar signals such as photoplethysmographic (PPG) pulse amplitudes of bilateral fingertips can reflect diabetes status is unknown. From a middle-to-old-aged population free of prior cardiovascular disease, we selected the unaffected (no type 2 diabetes, $n$ = 36), the well-controlled diabetes (glycated hemoglobin (HbA1c) <8%, $n$ = 30), and the poorly- controlled diabetes (HbA1c ≥8%, $n$ = 26) groups. MC-ApEn indexes were calculated from simultaneous consecutive 1500 PPG pulse amplitudes signals of bilateral index fingertips. The average of scale factors 1–5 ($MC\text{-}ApEn_{SS}$) and of scale factors 6–10 ($MC\text{-}ApEn_{LS}$) were defined as the small- and large-scales MC-ApEn, respectively. The $MC\text{-}ApEn_{LS}$ index was highest in the unaffected, followed by the well-controlled diabetes, and then the poorly-controlled diabetes (0.70, 0.62, and 0.53; all paired $p$-values were <0.05); in contrast, the $MC\text{-}ApEn_{SS}$ index did not differ between groups. Our findings suggested that the bilateral fingertips large-scale $MC\text{-}ApEn_{LS}$ index of PPG pulse amplitudes might be able to evaluate the glycemic status and detect subtle vascular disease in type 2 diabetes.

**Keywords:** multiscale cross-approximate entropy; photoplethysmographic wave amplitudes; type 2 diabetes

## 1. Introduction

Arterial stiffness is a major risk factor of clinical cardiovascular diseases (CVDs) [1]. In 2004, the difference in blood pressure acquired through the two upper arms was reported to reflect the risk of arteriosclerosis [2]. Another study demonstrated that inter-arm blood pressure differences (IABPDs) over 10 mmHg were highly associated with subclavian artery stenosis at the lower blood pressure site, and moreover, an IABPD over 15 mmHg may implicate peripheral vascular disease,

CVD, and be correlated with the associated mortalities [3]. According to the latest guideline from the European Society of Cardiology, a consistent difference in systolic blood pressure between two arms over 10 mmHg is associated with increased cardiovascular risk [4].

Systemic conditions such as aging and diabetes mellitus are known causes of arterial stiffness despite their differences in disease mechanisms [5]. Aging causes medial degeneration characterized by collagen and calcium deposits as well as fragmentation of elastin lamellae in the medial layer as a result of upregulation of proteolytic enzymes and possible repetitive cyclic stress on the arterial wall over a life span [6]. Diabetes mellitus is a chronic disease known to enhance the production of advanced glycation end-products that causes collagen crosslinking in the arterial medial layer which has been shown to be a significant contributor to arterial stiffness [7].

Although the measurement of IABPD may be a good surrogate for arteriosclerosis among individuals with older ages or type 2 diabetes, it is sometimes limited by the requirement of simultaneously assessing blood pressures at both arms with automatic devices and multiple readings to prevent overestimation and observer bias. Therefore, several digital cardiovascular signals rather than blood pressure have been used to evaluate arteriosclerosis in diabetes. Pincus et al. proposed that cross-approximate entropy (C-ApEn) can effectively evaluate the biological asynchrony between two different signal series [8]. Previously, we also showed the multiscale cross-approximate entropy (MC-ApEn) of electrocardiographic (ECG) R-R intervals with left finger photoplethysmographic (PPG) transit times and pulse amplitudes, and the large-scale multiscale entropy (MSE) of PPG pulse amplitudes correlating well with diabetes status [9,10]. Since PPG pulse amplitudes are related to arterial blood volume, pressures, and resistance, we hypothesized that MC-ApEn between two similar physiological signals such as PPG pulse amplitudes of bilateral fingertips may be practical to detect the presence of arteriosclerosis among individuals with older age or diabetes.

## 2. Methods

### *2.1. Study Population*

Between July 2009 and October 2010, we prospectively recruited 102 women and men with middle to old ages (range: 45–80 years) from the Ministry of Health and Welfare Hualien Hospital for PPG examinations of bilateral index fingertips. Of this population, 10 participants were excluded for a history of coronary heart disease, ischemic stroke, heart failure, chronic atrial fibrillation, peripheral arterial disease, or permanent pacemaker implantation, leaving a sample of 92 individuals for the MC-ApEn analysis. Diabetes mellitus was defined as fasting glucose $\geq$126 mg/dL or glycated hemoglobin (HbA1c) >6.5%, or the use of hypoglycemic medications. Of these, 36 participants did not have type 2 diabetes (the unaffected group), 30 had HbA1c <8% (the well-controlled diabetes group), and 26 had HbA1c $\geq$8% (the poorly-controlled diabetes group). This study was reviewed and approved by the Institutional Review Board of Hualien Hospital and National Dong-Hwa University. Each patient signed an informed consent.

### *2.2. Study Protocol*

All measurements and medical histories were taken in the morning (i.e., 8:30–10:30 a.m.). Demographic, anthropometric, and laboratory data for the analysis were obtained at the clinic visit. Body mass index was defined as body weight (kg)/height (m) squared. Blood pressure was measured once over the left arm of the supine participants by an automated oscillometric device (BP3AG1, Microlife, Taipei, Taiwan) with an appropriate cuff size. Concentrations of total cholesterol, low-density lipoprotein cholesterol, high-density lipoprotein cholesterol, and triglycerides were measured from blood samples obtained after a 12-h fast. The subjects were asked to refrain from caffeine-containing beverages and theophylline-containing medications for 12 h before each hospital visit. In addition, to minimize potential erroneous readings from the infrared sensors arising from involuntary vibrations of the examinees and a low environmental temperature possibly resulting in constriction of the

peripheral vessels, all subjects underwent blood sampling before data acquisition and were allowed to relax in a supine position for 10 min in a quiet room with temperature control at 26 ± 1 °C. Six-channel ECG-based pulse wave velocity (PWV) was obtained through simultaneous acquisition of ECG and PPG pulse signals from bilateral index fingertips for 30 min, and was averaged for the analysis [11,12].

### *2.3. Calculation of PPG Pulse Amplitudes Series from Bilateral Fingertips*

The PPG infrared sensors were simultaneously applied to bilateral index fingertips of the subjects for the acquisition of data. After being processed through an analog-to-digital converter (USB-6009 DAQ, National Instruments, Austin, TX, USA) at a sampling frequency of 500 Hz, the digitized signals were stored on a computer and analyzed by Matlab 7.7 software (MathWorks, Natick, MA, USA) [9]. The potential difference between the peak and the valley—which was post to the peak—was defined as the pulse amplitude of PPG signals (Figure 1). We simultaneously retrieved 1500 consecutive PPG pulse amplitudes of the left fingertip, shown as $\mathrm{PPGA_L}$ = {$\mathrm{PPGA_L}$(1), $\mathrm{PPGA_L}$(2), $\mathrm{PPGA_L}$(3), ..., $\mathrm{PPGA_L}$(n)} and those of right fingertip as $\mathrm{PPGA_R}$ = {$\mathrm{PPGA_R}$(1), $\mathrm{PPGA_R}$(2), $\mathrm{PPGA_R}$(3), ..., $\mathrm{PPGA_R}$(n)}, where $n$ = 1500 from each participant.

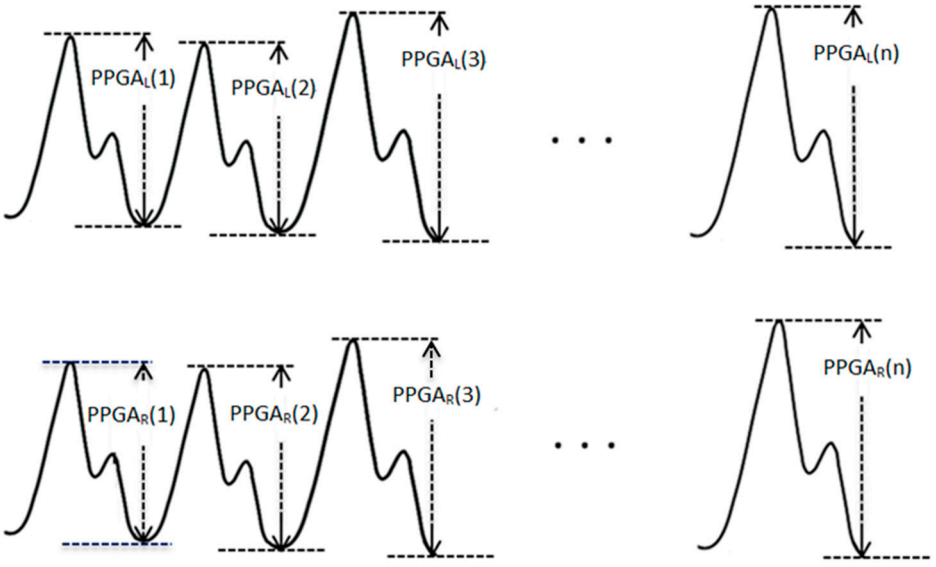


**Figure 1.** Photoplethysmograph pulse amplitude (PPGA) of left index finger ($\mathrm{PPGA_L}$) and right index finger ($\mathrm{PPGA_R}$) were simultaneously acquired from PPGA (1) to PPGA (1500).

Due to a trend within physiological signals [13], nonzero means may be included; therefore, we used empirical mode decomposition (EMD) [14] to deconstruct the {$\mathrm{PPGA_L}(i)$} and {$\mathrm{PPGA_R}(j)$} series, thereby eliminating the trend from the original series. We then normalized the {$\mathrm{PPGA_L}(i)$} and {$\mathrm{PPGA_R}(j)$} series, as shown in (1). In these equations, $SD_{\mathrm{PPGA_L}}$ and $SD_{\mathrm{PPGA_R}}$ represent the standard deviations of series {$\mathrm{PPGA_L}(i)$} and {$\mathrm{PPGA_R}(j)$}, respectively. $\overline{\mathrm{PPGA_L}}$ and $\overline{\mathrm{PPGA_R}}$ represent the mean of series {$\mathrm{PPGA_L}(i)$} and {$\mathrm{PPGA_R}(j)$}, respectively. Irregularity analysis was performed on the normalized results, $\mathrm{nPPGA_L}(i)$ and $\mathrm{nPPGA_R}(j)$.

$$\begin{aligned} \mathrm{nPPGA_L}(i) &= \frac{\mathrm{PPGA_L}(i) - \overline{\mathrm{PPGA_L}}}{SD_{\mathrm{PPGA_L}}} \\ \mathrm{nPPGA_R}(j) &= \frac{\mathrm{PPGA_R}(j) - \overline{\mathrm{PPGA_R}}}{SD_{\mathrm{PPGA_R}}} \end{aligned} \quad (1)$$

### *2.4. C-ApEn of Bilateral Fingertips PPG Pulse Amplitudes*

Previous studies have used C-ApEn—an improved analysis method of approximate entropy [15,16]—to analyze two different synchronous physiological time series, define their relationship, and calculate the irregularity within that relationship [8,17]. This method utilizes the dynamic changes between the two series to evaluate the physiological system. Similarities between changes in the two series can be used to observe the regulatory mechanisms in the physiological system. To obtain a deeper understanding of the irregularity of the physiological system, we utilized $\mathrm{nPPGA_L}$ and $\mathrm{nPPGA_R}$ series to calculate the C-ApEn, using (6). The details of the whole algorithm are as follows [18].

*Step 1.* For a given $m$, for two sets of $m$-vectors,

$$\begin{array}{l} \mathrm{x}(i) \equiv [\mathrm{nPPGA_L}\ (i)\ \mathrm{nPPGA_L}\ (i+1) \cdots \mathrm{nPPGA_L}\ (i+m-1)],\ 1 \le i \le N-m+1,\ \mathrm{i} \in \mathrm{N} \\ \mathrm{y}(j) \equiv [\mathrm{nPPGA_R}\ (j)\ \mathrm{nPPGA_R}\ (j+1) \cdots \mathrm{nPPGA_R}\ (j+m-1)],\ 1 \le j \le N-m+1,\ j \in \mathrm{N}. \end{array} \quad (2)$$

*Step 2.* Define the distance between the vectors $\mathbf{x}(i)$ and $\mathbf{y}(j)$ as the maximum absolute difference between their corresponding elements as follows:

$$d\ [\mathrm{x}(i),\ \mathrm{y}(j)] = \max\ [|\mathrm{nPPGA_L}\ (i+k-1) - \mathrm{nPPGA_R}\ (i+k-1)|] \quad (3)$$

*Step 3.* With the given matrix $\mathbf{x}(i)$ which refers to $\mathrm{nPPGA_L}$ (where $i$ = 1 to $N-m+1$), find the value of $d[\mathbf{x}(i), \mathbf{y}(j)]$ (where $j$ = 1 to $N-m+1$) that is smaller than or equal to $r$ and the ratio of this number to the total number of $m$-vectors ($N-m+1$). That is, let $N^m_{\mathrm{nPPGA_L nPPGA_R}}(i)$ equal the number of $\mathbf{y}(j)$ satisfying the requirement $d[\mathbf{x}(i), \mathbf{y}(j)] \leqq r$; then

$$C^m_{\mathrm{nPPGA_L nPPGA_R}}(i) = \frac{N^m_{\mathrm{nPPGA_L nPPGA_R}}(i)}{N-m+1} \quad (4)$$

$C^m_{\mathrm{nPPGA_L nPPGA_R}}(i)$ measures the frequency of the $m$-point $\mathrm{nPPGA_R}$ pattern being similar (within a tolerance of $\pm r$) to the $m$-point $\mathrm{nPPGA_L}$ pattern formed by $\mathbf{x}(i)$.

*Step 4.* Average the logarithm of $C^m_{\mathrm{nPPGA_L nPPGA_R}}(i)$ over $i$ to obtain $\varnothing^m_{\mathrm{nPPGA_L nPPGA_R}}(r)$ as follows:

$$\varnothing^m_{\mathrm{nPPGA_L nPPGA_R}}(r) = \frac{1}{N-m+1} \sum_{i=1}^{N-m+1} ln\ C^m_{\mathrm{nPPGA_L nPPGA_R}}(i) \quad (5)$$

*Step 5.* Increase $m$ by 1 and repeat Steps 1–4 to obtain $C^{m+1}_{\mathrm{nPPGA_L nPPGA_R}}(i)$ and $\varnothing^{m+1}_{\mathrm{nPPGA_L nPPGA_R}}(r)$.

*Step 6.* Finally, take $\mathrm{C-ApEn}_{\mathrm{nPPGA_L nPPGA_R}}(m,\ r) = \lim_{N\to\infty}[\varnothing^m_{\mathrm{nPPGA_L nPPGA_R}}(r) - \varnothing^{m+1}_{\mathrm{nPPGA_L nPPGA_R}}(r)]$. For $N$-point data, the estimate is

$$\mathrm{C\text{-}ApEn}_{\mathrm{nPPGA_L nPPGA_R}}(N, m,\ r) = [\varnothing^m_{\mathrm{nPPGA_L nPPGA_R}}(r) - \varnothing^{m+1}_{\mathrm{nPPGA_L nPPGA_R}}(r)] \quad (6)$$

where $m$ represents the chosen vector dimension, $r$ represents a tolerance range, and $N$ is the data length. From Pincus's publication, in order to effectively distinguish two data series by cross-approximate entropy, it would be better to set $N \geq 1000$, $m \geq 2$, and $r \geq 0.1$ [17]. To ensure efficiency and accuracy of calculation, the parameters of this study were set at $N$ = 1500, $m$ = 2, and $r$ = 0.15 multiplied by the standard deviation of the time series of $\mathrm{nPPGA_L}$.

### *2.5. Multiple Temporal Scale Analysis Used in MC-ApEn*

Multiple analysis involves the use of a scale factor $\tau$ ($\tau$ = 1, 2, 3, ..., $n$), which is selected according to a 1-D series of consecutive cycles. This factor enables the application of a coarse-graining process capable of deriving a new series prior to the calculation of entropy in each new individual series [14].

Using this approach, we performed coarse-graining on the normalized 1-D consecutive cycles of the $nPPGA_L(i)$ and $nPPGA_R(j)$ series based on scale factor $\tau$, thereby obtaining the series $nPPGA_L(i)$ and $nPPGA_R(j)$ as shown in (7). We then calculated as follows:

$$\begin{aligned} nPPGA_L(u)^{(\tau)} &= \frac{1}{\tau} \sum_{i=(u-1)\tau+1}^{u\tau} nPPGA_L(i),\ 1 \le u \le \frac{1500}{\tau},\ u \in N \\ nPPGA_R(u)^{(\tau)} &= \frac{1}{\tau} \sum_{j=(u-1)\tau+1}^{u\tau} nPPGA_R(j),\ 1 \le u \le \frac{1500}{\tau},\ u \in N \end{aligned} \tag{7}$$

Repeat Steps 1–7 to calculate the MC-ApEn index in scales 1–10. The values of $C\text{–}ApEn_{nPPGA_L nPPGA_R}(\tau)$ were obtained from a range of scale factors between 1 and 10 using the MC-pEn data analysis method. The summation values of $C\text{–}ApEn_{nPPGA_L nPPGA_R}(\tau)$ between scale factors 1 and 5 were defined as small scales [19]. The sum of C-ApEn between scale factors 1 and 5 was defined as $MC\text{-}ApEn_{SS}$ in (8).

$$MC\text{-}ApEn_{SS} = \sum_{\tau=1}^{5} C\text{-}ApEn_{nPPGA_L nPPGA_R}(\tau) \tag{8}$$

The summation values of $C\text{-}ApEn_{nPPGA_L nPPGA_R}(\tau)$ between scale factors 6 and 10 were defined as large scales [19]. The sum of C-ApEn between scale factors 6 and 10 was defined as $MC\text{-}ApEn_{LS}$ in (9).

$$MC\text{-}ApEn_{LS} = \sum_{\tau=6}^{10} C\text{-}ApEn_{nPPGA_L nPPGA_R}(\tau) \tag{9}$$

The sum of C-ApEn from scale factors 1 to 10 was defined as $MC\text{-}ApEn_{AVERAGE}$.

### *2.6. MSE of Unilateral Fingertip PPGA Pulse Amplitude*

To assess the complexity of unilateral fingertip PPGA series, sample entropy was used for multiscale analysis [16]. Since our previous study showed similar MSE levels of 1500 PPG pulse amplitudes between right and left fingertip in both unaffected individuals and those with diabetes [20], the left fingertip MSE was to be the representative for the analysis. The results of sample entropy between scale factors 1 and 5 were defined as small scales, and those between scale factors 6 and 10 were defined as large scales. The sum of MSE in small scales of $PPGA_L$ series was defined as $MSE_{SS}$, and the sum of MSE in large scales of $PPGA_L$ series was defined as $MSE_{LS}$.

### *2.7. Statistical Analysis*

Average values were expressed as mean ± standard deviation. Significant differences in anthropometric, hemodynamic, and computational parameters (i.e., $MC\text{-}ApEn_{LS}$ and $MC\text{-}ApEn_{SS}$) between different groups were determined using an independent sample *t*-test when the analysis data were normally distributed, and if the analysis data were not normally distributed, we used the nonparametric Mann-Whitney *U* test. Pearson's correlation test was performed to study the correlations of ECG-PWV, hemodynamic parameters, and serum biochemical data with MC-ApEn. A subcohort consisting of three age-matched groups (the unaffected, $n$ = 19; the well-controlled diabetes, $n$ = 28; and the poorly-controlled diabetes, $n$ = 23) was used for a sensitivity test. Statistical package for social sciences software (SPSS, version 14.0 for Windows) was used for all statistical analysis. A $p$-value less than 0.05 was considered statistically significant.

## 3. Results

The baseline characteristics of each group are shown in Table 1. Compared with the unaffected group, the diabetes group had relatively older ages and greater waist sizes, lower serum high-density lipoprotein cholesterol, HbA1c levels, and greater ECG-PWV. As compared with the well-controlled

diabetes, the poorly-controlled diabetes had higher serum triglycerides, low-density lipoprotein cholesterol, and HbA1c levels. The $MSE_{ss}$ did not differ between groups, nor did the MC-$ApEn_{SS}$ differ. The $MSE_{LS}$ in the poorly-controlled diabetes was lower than that in the unaffected, but similar to that in the well-controlled diabetes. In contrast, the MC-$ApEn_{LS}$ index was highest in the unaffected, followed by the well-controlled diabetes, and then the poorly-controlled diabetes (0.70, 0.62, and 0.53; all paired *p*-values were <0.05).

**Table 1.** Baseline characteristics of non-diabetic participants (Unaffected), those with well-controlled diabetes (glycated hemoglobin (HbA1c) <8%), and those with poorly-controlled diabetes (HbA1c ≥8%).

| | **Unaffected** | **Diabetes, HbA1c <8%** | **Diabetes, HbA1c ≥8%** |
|---|---|---|---|
| | ***n* = 36** | ***n* = 30** | ***n* = 26** |
| Men (%) | 15 (41.7%) | 18 (60%) | 15 (57.7%) |
| Age, y | 55.08 ± 8.47 | 67.93 ± 7.75 $^{++}$ | 60.73 ± 7.28 $^{*,a}$ |
| Height, cm | 161.44 ± 8.06 | 161.86 ± 8.68 | 161.35 ± 6.99 |
| Weight, kg | 63.99 ± 11.87 | 70.32 ± 13.76 | 73.27 ± 11.52 * |
| Waist circumference, cm | 83.73 ± 10.72 | 93.52 ± 10.29 $^{++}$ | 95.6 ± 11.03 ** |
| BMI, kg/m$^2$ | 24.43 ± 3.47 | 26.17 ± 6.04 | 28.18 ± 4.397 * |
| SBP, mmHg | 120.77 ± 15.51 | 122.28 ± 15.59 | 121.89 ± 30.67 |
| DBP, mmHg | 75.77 ± 10.40 | 72.52 ± 10.71 | 72.96 ± 18.13 |
| Pulse pressure, mmHg | 43.75 ± 13.75 | 49.76 ± 11.31 | 48.92 ± 17.07 |
| Total Cholesterol, mg/dL | 193.67 ± 35.09 | 167.42 ± 27.18 | 198.6 ± 47.21 $^{a}$ |
| Triglycerides mg/dL | 111.44 ± 86.86 | 123.08 ± 43.89 | 169.54 ± 91.98 $^{*,a}$ |
| HDL-Cholesterol, mg/dL | 49.94 ± 16.63 | 40.65 ± 10.84 $^{+}$ | 40.25 ± 9.21 * |
| LDL-Cholesterol, mg/dL | 116.14 ± 30.15 | 95.04 ± 23.59 $^{+}$ | 122.61 ± 31.93 $^{a}$ |
| Cholesterol/HDL ratio | 4.24 ± 1.403 | 4.64 ±2.89 $^{+}$ | 5.09 ±1.44 * |
| FPG, mg/dL | 104.94 ± 21.996 | 124.92 ± 22.98 $^{+}$ | 176.17 ± 60.595 $^{**,aa}$ |
| HbA1c, % | 5.94 ± 0.41 | 7.16 ± 0.38 $^{++}$ | 9.54 ± 1.73 $^{**,aa}$ |
| ECG-PWV, cm/s | 5.31±0.33 | 5.71±0.21 $^{+}$ | 5.75 ± 0.49 * |
| $MSE_{ss}$ | 1.23 ± 0.36 | 1.12 ± 0.36 | 1.14 ± 0.41 |
| $MSE_{LS}$ | 1.56 ± 0.44 | 1.39 ± 0.39 | 1.32 ± 0.38 * |
| MC-$ApEn_{SS}$ | 0.48 ± 0.08 | 0.47 ± 0.13 | 0.45 ± 0.12 |
| MC-$ApEn_{LS}$ | 0.70 ± 0.08 | 0.62 ± 0.14 $^{+}$ | 0.53 ± 0.16 $^{**,a}$ |

Continuous variables are expressed as mean ± standard deviations, and categorical variables as number (percentage). Abbreviations: BMI, body mass index; DBP, diastolic blood pressure; ECG-PWV, electrocardiographic pulse wave velocity; FPG, fasting plasma glucose; HbA1c, hemoglobin A1c; HDL-C, high-density lipoprotein cholesterol; LDL-C, low-density lipoprotein cholesterol; LS, large scales; MC-ApEn, multiscale cross-approximate entropy; MSE, multiscale entropy; SBP, systolic blood pressure; SS, small scales. Unaffected vs. Diabetes, HbA1c <8% $^{+}$ $p < 0.05$; $^{++}$ $p < 0.001$. Unaffected vs. Diabetes, HbA1c ≥8% * $p < 0.05$; ** $p < 0.001$. Diabetes, HbA1c <8% vs. Diabetes, HbA1c ≥8% $^{a}$ $p < 0.05$; $^{aa}$ $p < 0.001$.

Table 2 shows the correlations of MC-ApEn with hemodynamic parameters, serum glycemic index, lipid profiles, and ECG-PWV. MC-$ApEn_{AVERAGE}$ was inversely correlated with body weight, waist circumference, body mass index, and HbA1c, and borderline inversely correlated with fasting plasma glucose and ECG-PWV. Of these variables, HbA1c was the strongest one associated with MC-$ApEn_{AVERAGE}$ ($r = -0.316$). Similarly, MC-$ApEn_{LS}$ was inversely correlated with body weight, waist circumference, body mass index, HbA1c, fasting plasma glucose, and ECG-PWV. ECG-PWV and HbA1c were moderately correlated with MC-$ApEn_{LS}$ ($r = -0.423$ and $-0.397$, respectively). In contrast, MC-$ApEn_{SS}$ was not correlated with any of these variables except body mass index ($r = -0.232$).

Figure 2 shows the MC-ApEn index at each scale factor of the three groups. Generally, the unaffected group had the highest MC-ApEn and the poorly-controlled diabetes group had the lowest MC-ApEn across scale factors 6–10 (large scales). However, the unaffected group had the lowest MC-ApEn compared with the two diabetes groups at scale factor 1, but the average of MC-ApEn across scales 1–5 (small scales) did not differ between groups.

**Table 2.** Correlations of ECG-PWV, hemodynamic, and serum biochemical data with MC-ApEn.

| | $\mathbf{MC\text{-}ApEn_{AVERAGE}}$ | | $\mathbf{MC\text{-}ApEn_{SS}}$ | | $\mathbf{MC\text{-}ApEn_{LS}}$ | |
|---|---|---|---|---|---|---|
| | *r* | *p* | *r* | *p* | *r* | *p* |
| Age, year | −0.051 | 0.626 | 0.058 | 0.580 | −0.126 | 0.233 |
| Height, cm | −0.020 | 0.851 | 0.024 | 0.825 | −0.049 | 0.645 |
| Weight, kg | −0.246 | 0.019 | −0.148 | 0.162 | −0.268 | 0.010 |
| Waist circumstance, cm | −0.262 | 0.013 | −0.144 | 0.178 | −0.296 | 0.005 |
| BMI, kg/m$^2$ | −0.282 | 0.007 | −0.232 | 0.027 | −0.259 | 0.013 |
| SBP, mmHg | 0.046 | 0.665 | 0.136 | 0.203 | −0.032 | 0.761 |
| DBP, mmHg | 0.092 | 0.387 | 0.045 | 0.673 | 0.108 | 0.309 |
| Pulse pressure, mmHg | −0.029 | 0.788 | 0.149 | 0.160 | −0.159 | 0.133 |
| HbA1c, % | −0.316 | 0.002 | −0.124 | 0.238 | −0.397 | <0.001 |
| Total cholesterol, mg/dL | 0.050 | 0.649 | 0.055 | 0.619 | 0.036 | 0.743 |
| Triglycerides, mg/dL | −0.189 | 0.085 | −0.072 | 0.516 | −0.237 | 0.030 |
| HDL-Cholesterol, mg/dL | 0.129 | 0.244 | 0.058 | 0.601 | 0.157 | 0.157 |
| LDL-Cholesterol, mg/dL | 0.046 | 0.682 | 0.001 | 0.991 | 0.071 | 0.528 |
| FPG, mg/dL | −0.210 | 0.058 | −0.049 | 0.665 | −0.291 | 0.008 |
| Cholesterol/HDL-C | −0.018 | 0.871 | 0.039 | 0.728 | −0.058 | 0.603 |
| ECG-PWV, cm/s | −0.309 | 0.056 | −0.071 | 0.669 | −0.423 | 0.007 |

Abbreviations: BMI, body mass index; DBP, diastolic blood pressure; ECG-PWV, electrocardiographic pulse wave velocity; FPG, fasting plasma glucose; HbA1c, hemoglobin A1c; HDL, high-density lipoprotein; LDL, low-density lipoprotein; LS, large scales; MC-ApEn, multiscale cross-approximate entropy; SBP, systolic blood pressure; SS, small scales.

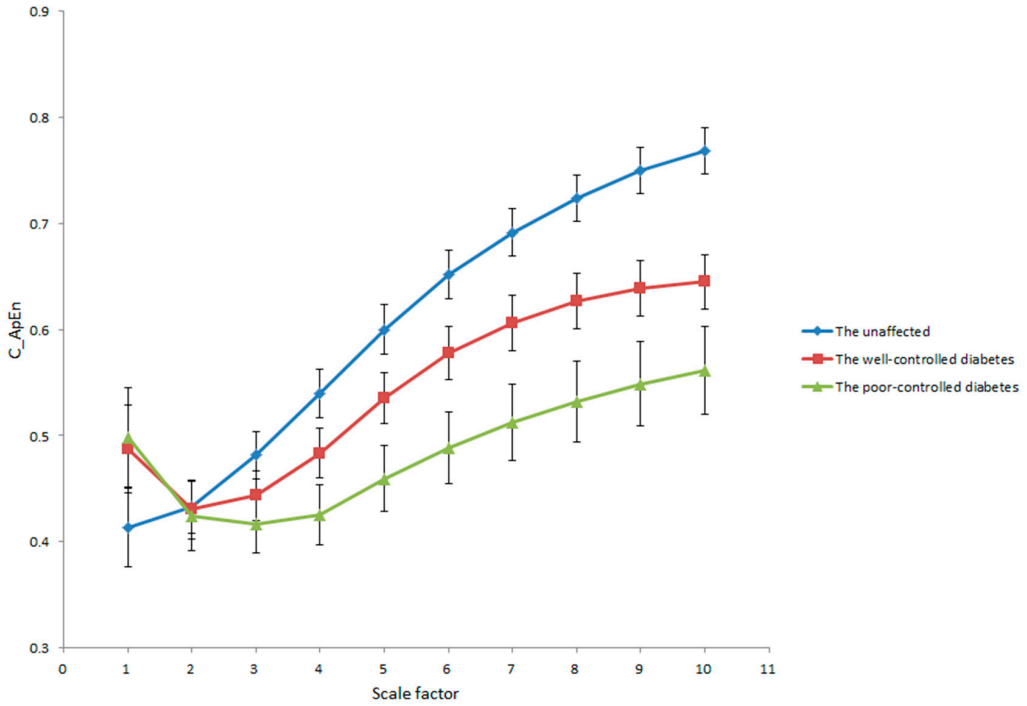


**Figure 2.** The MC-ApEn of bilateral index fingers with the standard error (vertical bar) of the unaffected (solid blue line), the well-controlled diabetes (solid red line), and the poorly-controlled diabetes (solid green line) at each scale factor.

*MC-ApEn in the Three Age-Matched Groups for a Sensitivity Test*

The baseline characteristics of the three age-matched groups in the subcohort are shown in the Table S1. The results for MSE and MC-ApEn of PPG pulse signals in the subcohort were in line with those in the original cohort. The diabetes and the unaffected groups could be differentiated by both

$MSE_{LS}$ and MC-$ApEn_{LS}$, whereas the glycemic control status in the diabetes group could only be differentiated by MC-$ApEn_{LS}$. The MC-ApEn of the three age-matched groups at scale factors 1–10 are shown in the Figure S1, and the trend was similar to those from the original cohort in Figure 2.

## 4. Discussion

Our principal findings are that bilateral fingertips PPG pulse amplitudes could be used for MC-ApEn analysis to evaluate arteriosclerosis and type 2 diabetes status in middle-to-old-aged individuals. In addition, the large-scale MC-$ApEn_{LS}$ index had a moderate inverse association with hyperglycemia and ECG-PWV—a marker of arteriosclerosis—in type 2 diabetes. Moreover, the large-scale MC-$ApEn_{LS}$ index was superior to the large-scale $MSE_{LS}$ of unilateral left finger PPG pulse signals to differentiate the glycemic status in those with type 2 diabetes.

The correlation between blood pressure and digital volume pulse was first studied in 1955 [21]. The parameters of waveform contour analysis such as reflection index, crest time, and stiffness index were adopted in the arterial stiffness study [22]. Moreover, digital volume pulse has been further found to reflect cardiovascular and metabolic risks [17]. The feasibility and sensitivity of using digital volume pulse in the assessment of cardio-metabolic risks according to its complexity between both sides of the body, however, have not been reported. On the other hand, it has been previously shown to be related to peripheral pressure pulse by a transfer function independent of the effects of hypertension or anti-hypertensive agents [23]. Therefore, the present study not only tested the hypothesis that computation on the bilateral fingertips PPG pulse amplitudes complexity could stratify the status of glycemic control in type 2 diabetes, but also examined the sensitivity of MC-ApEn to detect demographic, hemodynamic, and biochemical parameters contributing to arteriosclerosis in middle-to-old-aged individuals [12,21].

The concept of MC-ApEn between two similar signals of bilateral fingertips PPG pulse amplitudes was like the beats-by-beats asynchrony of IABPD and peripheral arterial resistance of bilateral upper extremities. Theoretically, the MC-ApEn index at scale factor 1 in each group should be close to the average of IABPD measured for 1500 consecutive times and the mean ECG-PWV from bilateral fingertips. Our study revealed that the MC-ApEn index at scale factor 1 was correlated with ECG-PWV in each group (the unaffected vs. the poorly-controlled diabetes, $p = 0.055$). When compared with the means of simultaneous blood pressure measurement using sphygmomanometer cuffs on upper arms, PPG has the advantages of being more comfortable, economical, and also allows continuous measurement without the need for repeated pressure cuff inflations.

Previously, we used MSE analysis of PPG pulse amplitudes of left index fingertip in middle-to-old-aged individuals and revealed that the large-scale MSE index (scale factors: 4–6) was higher in the healthy controls than that in patients with type 2 diabetes. In contrast, the small-scale MSE index (scale factors: 1–3) between the healthy individuals and diabetic patients did not differ. In addition, the MC-ApEn analysis between left fingertip PPG pulse amplitudes with other different physiological signals of ECG R-R intervals demonstrated similar results. Costa et al. and Trunkvalterova et al. have demonstrated that the small-scale MSE of heart rate variability—reflecting autonomic function—was decreased in diabetes, and similarly, the large-scale MSE of pulse transit times—a surrogate of peripheral arteriosclerosis—was also lower in diabetes [24,25]. The MSE index of unilateral finger PPG pulse amplitudes may reflect peripheral vascular health of the tested upper extremity side. Obviously in the present study, the MC-ApEn index was more sensitive than the MSE index in detecting the severity of systemic arterial stiffness if either side of the upper extremities artery or thoracic aorta was affected by diabetic complications which were related to the glycemic control status.

The strengths of our study include the availability of large numbers of serial PPG pulse amplitude signals of bilateral fingertips and the availability of a wide range of vascular risk parameters. In addition, the issue that the MC-ApEn may be influenced by the age difference between groups in the original cohort could be much convinced because the sensitivity test using three age-matched

groups from the subcohort shows consistent results. In contrast, there were some limitations in using PPG sensors for detecting PPG signals. Firstly, readings from infrared sensors may be affected by skin pigmentation, tissue characteristics, and blood flow in the measured area [26]. Second, the signals may also be disturbed by involuntary vibrations of the subjects being examined. Finally, the measurement may also be affected by a decreased environmental temperature that tends to result in peripheral vessel constriction. The influence of this condition can be minimized by maintaining a room temperature at $26 \pm 1$ °C at the time of measurement.

In conclusion, our findings suggest that the large-scale MC-ApEn index of bilateral fingertips PPG pulse amplitudes was better than the MSE index of unilateral fingertip PPG pulse amplitudes for the evaluation of glycemic control status and detecting early arteriosclerosis in middle-to-old-aged individuals with or without diabetes.

**Supplementary Materials:** The following are available online at www.mdpi.com/1099-4300/19/4/145/s1, Table S1: Baseline Characteristics of the Three Age-Matched Groups (Unaffected, Diabetes, HbA1c <8% and Diabetes, HbA1c ≥8%) from the Subcohort, Figure S1: The MC-ApEn of bilateral index fingers with the standard error (vertical bar) of the age-matched unaffected (solid blue line), the well-controlled diabetes (solid red line), and the poorly-controlled diabetes (solid green line) at each scale factor, respectively.

**Acknowledgments:** This work was supported by the research grants from the Ministry of Science and Technology, Taiwan (Grant No. MOST 104-2221-E-259-014, and MOST 105-2221-E259-007).

**Author Contributions:** Hsien-Tsai Wu and Cheng-Chan Yang conceived and designed the experiments; Hsien-Tsai Wu performed the experiments; Shiao-Chiang Chu analyzed the data; Bagus Haryadi and Chieh-Ming Yang made critical comments; Gen-Min Lin and Cheuk-Kwan Sun wrote the paper.

**Conflicts of Interest:** The authors declare no conflict of interest.

## References

1. Blacher, J.; Guerin, A.P.; Pannier, B.; Marchais, S.J.; Safar, M.E.; London, G.M. Impact of aortic stiffness on survival in end-stage renal disease. *Circulation* **1999**, *99*, 2434–2439. [CrossRef] [PubMed]
2. Kimura, A.; Hashimoto, J.; Watabe, D.; Takahashi, H.; Ohkubo, T.; Kikuya, M.; Imai, Y. Patient characteristics and factors associated with inter-arm difference of blood pressure measurements in a general population in Ohasama, Japan. *J. Hypertens.* **2004**, *22*, 2277–2283. [CrossRef] [PubMed]
3. Clark, C.E.; Taylor, R.S.; Shore, A.C.; Ukoumunne, O.C.; Campbell, J.L. Association of a difference in systolic blood pressure between arms with vascular disease and mortality: A systematic review and meta-analysis. *Lancet* **2012**, *379*, 905–914. [CrossRef]
4. Task Force for the management of arterial hypertension of the European Society of Cardiology. 2013 ESH/ESC guidelines for the management of arterial hypertension. *Blood Press.* **2013**, *22*, 193–278.
5. Sun, C.K. Cardio-ankle vascular index (CAVI) as an indicator of arterial stiffness. *Integr. Blood. Press. Control* **2013**, *6*, 27. [CrossRef] [PubMed]
6. McEniery, C.M.; O'Shaughnessy, K.M.; Harnett, P.; Harnett, P.; Arshad, A.; Wallace, S.; Maki-Petaja, K.; McDonnell, B.; Ashby, M.J.; Brown, J.; et al. Variation in the human matrix metalloproteinase-9 gene is associated with arterial stiffness in healthy individuals. *Arterioscler. Thromb. Vasc. Biol.* **2006**, *26*, 1799–1805.
7. Corman, B.; Duriez, M.; Poitevin, P.; Heudes, D.; Bruneval, P.; Tedgui, A.; Levy, B.I. Aminoguanidine prevents age-related arterial stiffening and cardiac hypertrophy. *Proc. Natl. Acad. Sci. USA* **1998**, *95*, 1301–1306. [CrossRef] [PubMed]
8. Pincus, S.M. Approximate entropy in cardiology. *Herzschrittmachertherapie und Elektrophysiologie* **2000**, *11*, 139–150. [CrossRef]
9. Wu, H.T.; Liu, C.C.; Lo, M.T.; Hsu, P.C.; Liu, A.B.; Chang, K.Y.; Tang, C.J. Multiscale cross-approximate entropy analysis as a measure of complexity among the aged and diabetic. *Comput. Math. Methods Med.* **2013**, *2013*, 324325. [CrossRef] [PubMed]
10. Wu, H.T.; Lee, C.Y.; Liu, C.C.; Liu, A.B. Multiscale cross-approximate entropy analysis as a measurement of complexity between ECG R-R interval and PPG pulse amplitude series among the normal and diabetic subjects. *Comput. Math. Methods Med.* **2013**, *2013*, 231762. [CrossRef] [PubMed]
11. Liu, A.B.; Hsu, P.C.; Chen, Z.L.; Wu, H.T. Measuring pulse wave velocity using ECG and photoplethysmography. *J. Med. Syst.* **2011**, *35*, 771–777. [CrossRef] [PubMed]

12. Wu, H.T.; Hsu, P.C.; Liu, A.B.; Chen, Z.L.; Huang, R.M.; Chen, C.P.; Tang, C.J.; Sun, C.K. Six-channel ECG-based pulse wave velocity for assessing whole-body arterial stiffness. *Blood Press.* **2012**, *21*, 167–176. [CrossRef] [PubMed]
13. Wu, Z.; Huang, N.E.; Long, S.R.; Peng, C.K. On the trend, detrending, and variability of nonlinear and nonstationary time series. *Proc. Natl. Acad. Sci. USA* **2007**, *104*, 14889–14894. [CrossRef] [PubMed]
14. Huang, N.E.; Shen, Z.; Long, S.R.; Wu, M.C.; Shih, H.H.; Zheng, Q.; Yen, N.C.; Tung, C.C.; Liu, H.H. The empirical mode decomposition and the Hubert spectrum for nonlinear and non-stationary time series analysis. *Proc. R. Soc. A* **1998**, *454*, 903–995. [CrossRef]
15. Kreuzer, M.; Hentschke, H.; Antkowiak, B.; Schwarz, C.; Kochs, E.F.; Schneider, G. Cross-approximate entropy of cortical local field potentials quantifies effects of anesthesia—A pilot study in rats. *BMC Neurosci.* **2010**, *11*, 122. [CrossRef] [PubMed]
16. Pincus, S.; Singer, B.H. Randomness and degrees of irregularity. *Proc. Natl. Acad. Sci. USA* **1996**, *93*, 2083–2088. [CrossRef] [PubMed]
17. Pincus, S.M. Irregularity and asynchrony in biologic network signals. *Methods Enzymol.* **2000**, *321*, 149–182. [PubMed]
18. Yang, F.; Hong, B.; Tang, Q. Approximate entropy and its application to biosignal analysis. *Nonlinear Biomed. Signal Process.* **2001**, *2*, 72–79.
19. Cheng, D.; Tsai, S.J.; Hong, C.J.; Yang, A.C. Reduced physiological complexity in robust elderly adults with the APOE epsilon4 allele. *PLoS ONE* **2009**, *4*, e7733. [CrossRef] [PubMed]
20. Lin, G.M.; Haryadi, B.; Yang, C.M.; Chu, S.C.; Yang, C.C.; Wu, H.T. Discrepancies between conventional multiscale entropy and modified short-time multiscale entropy of photoplethysmographic pulse signals in middle- and old-aged individuals with or without diabetes. *Entropy* **2017**, *19*, 132. [CrossRef]
21. Currens, J.; Mcginty, J.; Khambatta, R.; Gordon, I. The effect of intravenous protoveratrine on digital pulse volume and digital skin temperature in hypertensive patients. *Circulation* **1955**, *11*, 440–446. [CrossRef] [PubMed]
22. Wu, H.T.; Liu, C.C.; Lin, P.H.; Chung, H.M.; Liu, M.C.; Yip, H.K.; Liu, A.B.; Sun, C.K. Novel application of parameters in waveform contour analysis for assessing arterial stiffness in aged and atherosclerotic subjects. *Atherosclerosis* **2010**, *213*, 173–177. [CrossRef] [PubMed]
23. Shadman, R.; Criqui, M.H.; Bundens, W.P.; Fronek, A.; Denenberg, J.O.; Gamst, A.C.; McDermott, M.M. Subclavian artery stenosis: Prevalence, risk factors, and association with cardiovascular diseases. *J. Am. Coll. Cardiol.* **2004**, *44*, 618–623. [CrossRef] [PubMed]
24. Costa, M.; Goldberger, A.L.; Peng, C.K. Multiscale entropy analysis of complex physiologic time series. *Phys. Rev. Lett.* **2002**, *89*, 068102. [CrossRef] [PubMed]
25. Trunkvalterova, Z.; Javorka, M.; Tonhajzerova, I.; Javorkova, J.; Lazarova, Z.; Javorka, K.; Baumert, M. Reduced short-term complexity of heart rate and blood pressure dynamics in patients with diabetes mellitus type 1: Multiscale entropy analysis. *Physiol. Meas.* **2008**, *29*, 817–828. [CrossRef] [PubMed]
26. Schultz-Ehrenburg, U.; Blazek, V. Value of quantitative photoplethysmography for functional vascular diagnostics. *Skin Pharmacol. Physiol.* **2001**, *14*, 316–323. [CrossRef]